DEVELOPMENT OF A REGENERATIVE SHOCK ABSORBER FOR A TWO WHEELER VEHICLE FOR ENERGY HARVESTING

Harish Vishwanathan[*]

Arun Kumar*

I ABSTRACT

A Regenerative shock absorber is designed and analyzed in this project. It converts variable frequency, repetitive intermittent linear displacement motion to useful electrical power. It uses the Faraday's law of electromagnetic induction and produces power through change in magnetic flux interacting with the coil winding. The shock absorber has the ability to convert the wasted vibration energy, which the vehicle encounters into useful power for charging batteries and other vehicle accessories. The device is capable of producing power with high efficiency with minimal weight penalty.

The regenerative shock absorber was mathematically modeled and the designing was done using the Pro E software. The design was then fabricated by using neodymium magnets for the magnetic field and copper coil acts as the conductor and transmits the induced power to the battery and electrical equipment through a rectifying circuit.

The road vibrations were transferred to the shock absorber, which produces a changing magnetic field and the voltage is induced in the coil whose magnitude was found using Lorentz Force calculation. The voltage produced is alternating and highly varying in magnitude. So a rectification and conditioning circuit was constructed whose output can be directly connected to a battery or other electrical appliances attached to the vehicle.

The magnetic field consists of neodymium ring magnets, which are more powerful than normal ferro magnets and spacers are made up of Stainless Steel, which are stacked on a Mild Steel rod. The copper coil is wounded on a stainless steel slotted tube and is given a very small clearance

---

[*] Department of Automobile Engineering, MIT, Anna University

between the magnet stack. An aluminum dust cover prevents the dust and water entering the circuit. The fabrication processes carried out for the above said parts are discussed.

The experiment was conducted by fitting the fabricated shock absorber in a two wheeler vehicle and the analysis of the device was done with the help of a Digital Storage Oscilloscope (DSO). The results and discussions are made in the later part of the report. The optimization done by intuitive and logical basis for better performance of the device is also discussed. The ability of this shock absorber to expand its presence to various domains of the vehicle and ways of increasing the overall power production are proposed in the future works.

II OBJECTIVE AND METHODOLOGY

2.1. Objective

The main objective of this project is to develop a regenerative shock absorber (RGSA) with a power capacity of 6 W. The project also targets the following objectives:

- Studying the performance of the device under various road conditions
- Improve the fabricated RGSA for optimizing power production

2.2. Methodology

The steps followed in development of regenerative shock absorber are:

- Collection of literatures and studying the background of similar devices
- Simulation of the RGSA using mathematical modeling
- Solid modeling of RGSA using Pro E
- Collecting suitable materials for fabricating the device
- Setting up the test bench for conducting experiments
- Study the device under various road conditions
- Research and develop the device for optimizing the power production
- Propose future works

A Monthly Double-Blind Peer Reviewed Refereed Open Access International e-Journal - Included in the International Serial Directories
Indexed & Listed at: Ulrich's Periodicals Directory ©, U.S.A., Open J-Gage as well as in Cabell's Directories of Publishing Opportunities, U.S.A.

International Journal of Management, IT and Engineering
http://www.ijmra.us

234

3. FUNDAMENTAL THEORIES OF ELECTROMAGNETISM

The fundamental entities of electromagnetic theory, necessary for understanding of the regenerative shock absorber, are introduced briefly below.

3.1 Fundamental Entities

3.1.1 Magnetic Field Intensity (H)

The magnetic field can be defined in many equivalent ways based on the effects it has on its environment. For instance, a particle having an electric charge, q, and moving in a B-field with a velocity, v, experiences a force, F, called the Lorentz force.

$$H = \frac{\mu_0 I}{4\pi} \int \frac{d\ell \times \hat{r}}{r^2} \qquad (3.1)$$

The integration is carried out over the circuit C. The unit vector $\vec{r1}$ and the distance r show the direction and distance respectively from the source to the point of observation. Magnetic field intensity is expressed in Am^{-1}.

3.1.2 Magnetic Induction (B)

Magnetic Induction is defined by the force it exerts on a conductor carrying a electrical current. It is related with the magnetic field intensity as:

$B = \mu. H$ (3.2)

where the constant μ is the permeability of the medium. Magnetic Induction is expressed in Tesla (T). The permeability of free space μ_o is $4\pi \times 10^{-7}$ Tm A^{-1}.

3.1.3 Right Hand Grip Rule

The direction of force on a charge or a current can be determined by the **right-hand rule**. Using the right hand and pointing the thumb in the direction of the moving positive charge or positive current and the fingers in the direction of the magnetic field the resulting force on the charge points outwards from the palm. The force on a negatively charged particle is in the opposite

A Monthly Double-Blind Peer Reviewed Refereed Open Access International e-Journal - Included in the International Serial Directories
Indexed & Listed at: Ulrich's Periodicals Directory ©, U.S.A., Open J-Gage as well as in Cabell's Directories of Publishing Opportunities, U.S.A.
International Journal of Management, IT and Engineering
http://www.ijmra.us

235

direction. If both the speed and the charge are reversed then the direction of the force remains the same. For that reason a magnetic field measurement (by itself) cannot distinguish whether there is a positive charge moving to the right or a negative charge moving to the left.
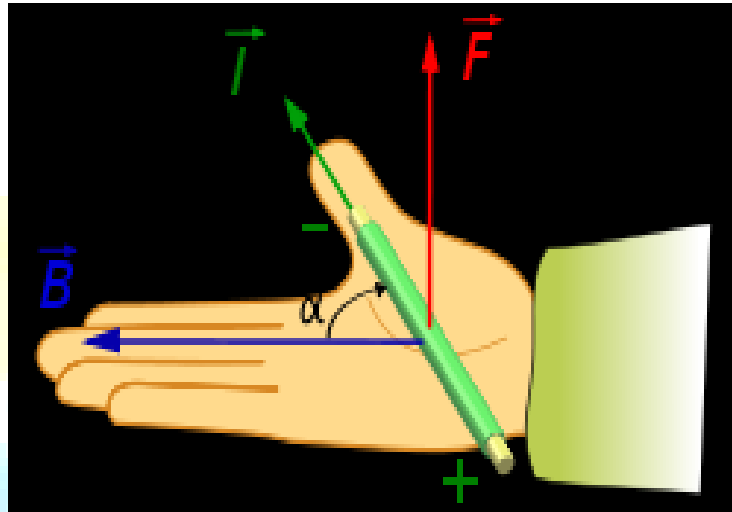

Fig 3.1: Right Hand Grip Rule

3.1.4 Magnetic Flux (φ)

The magnetic flux through a surface is

$$\phi = \int B.d\vec{a} \quad (3.3)$$

It is measured in weber (Wb)

3.1.5 Magnetization (M)

The magnetization M is the magnetic moment per unit volume at a given point in a medium. The magnetic moment is associated with the orbital and spinning motion of electrons. It has the same unit as the magnetic field intensity. The magnetization M and the magnetic field Intensity H contribute to the magnetic induction as

$$B = \mu_0(H + M) \quad (3.4)$$

This is called the field equation.

3.2 Fundamental Equations

The whole electromagnetic theory can be derived from Maxwell's four fundamental equations. Three of these will be necessary for the understanding of the theory in this work, namely:

$$\nabla.\mathbf{B} = 0 \qquad \textbf{(3.5)}$$

$$\nabla \textbf{x H} = \textbf{J}\,\frac{\partial D}{\partial t} \qquad \textbf{(3.6)}$$

$$\nabla \textbf{x E} = -\frac{\partial B}{\partial t} \qquad \textbf{(3.7)}$$

Equation (5) is also known as **Gauss' law.** It states that the net flux of B in any volume is zero. Unlike electrical field lines, magnetic field lines must be a closed continuous curve. This must always be taken into account in the design of the magnetic circuit of a generator.

In equation (6) J is the volume current density. The second term on the right hand side deals with the electric displacement D and will be neglected in all applications in this work. By using Stoke's theorem (6) can be rewritten as follows:

$$\oint H.\,d\hat{l} = \int J.\,d\hat{a} \quad \textbf{(3.8)}$$

This is also known as Ampere's law. It states that line integral of H over a closed curve C is equal to the current crossing the surface S bound by C. What is often the case is that the same current crosses the surface bounded by the curve C several times. With a solenoid, for example, C could follow the axis and then return outside the solenoid. The total current crossing the surface is then multiplied by the number of turns.

Equation (7) states that the curl of the electric field is equal to the negative time the derivative of the magnetic field. The equation can be rewritten by using the Stoke's theorem on the left hand side and eq (3) on the right hand side.

$$\mathbf{e} = -\frac{d\emptyset}{dt} \qquad \textbf{(3.9)}$$

This is the Faraday induction law for v x B field stating that the induced electromotance e (voltage) in a closed circuit is equal to the negative time derivative of the total flux bound by the circuit. The direction of the current induced in the circuit is such that it opposes, to a greater or lesser extent depending on the resistance of the circuit, the change in flux. If the closed circuit comprises N turns close together, each intercepting the same magnetic flux, then the

electromotances add up, resulting in an N times larger electromotance. Then Nϕ is called the flux linkage[1].

3.3 Ferromagnetic Materials

Ferromagnetic materials are magnetic dipoles and can reach very high levels of magnetization. The relative permeability μ of a medium describes how much better, compared with vacuum, the material leads magnetic flux. The permeability depends on the magnetization M of the material as follows:

$$\mu = \mu_o \left(1 + \frac{M}{H} \right) \quad (3.10)$$

Ferromagnetic materials have very high permeability and are therefore used in magnetic devices to lead the magnetic flux. The quota M/H is material dependent and is called susceptibility of the material. For a given material the relation between the magnetic field intensity H and the magnetization M is described by a magnetization curve.
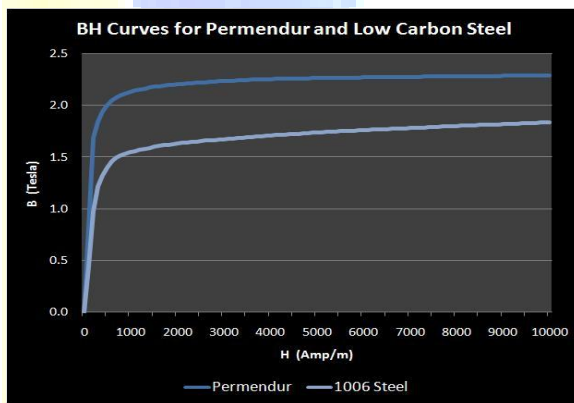
Fig 3.2: BH Curve for Steel

3.4 Linear Generator

3.4.1 Design Principle

A linear alternator is essentially a linear motor used as an electrical generator.

An alternator is a type of alternating current (AC) electrical generator. The devices are often physically equivalent. The principal difference is in how they are used and which direction the energy flows. An alternator converts mechanical energy to electrical energy, whereas a motor converts electrical energy to mechanical energy. Like most electric motors and electric generators, the linear alternator works by the principle of electromagnetic induction. However, most alternators work with rotary motion, whereas "linear" alternators work with "linear" motion (i.e. motion in a straight line).

When a magnet moves in relation to a coil of wire, this changes the magnetic flux passing through the coil, and thus induces the flow of an electric current, which can be used to do work. A linear alternator is most commonly used to convert reciprocating (i.e. back-and-forth) motion directly into electrical energy. This short-cut eliminates the need for a crank or linkage that would otherwise be required to convert a reciprocating motion to a rotary motion in order to be compatible with a rotary generator[3].
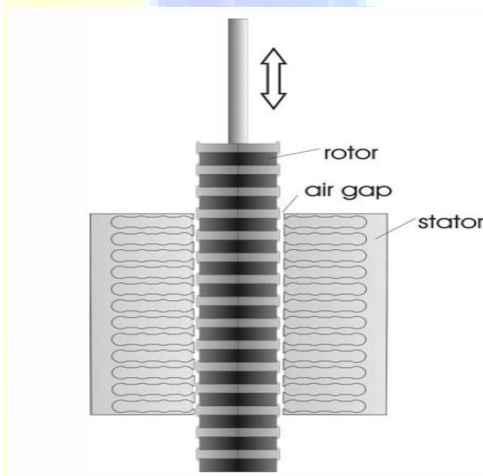

Fig 3.3: A two sided linear generator

2.4.2 Power Losses

The power losses in a generator consist of three parts:

1. Losses due to changing magnetic field
2. Resistive losses in the coil windings

3. Mechanical losses

Hysteresis losses

Hysteresis losses are the energy it takes to reverse the magnetization of the material and will only affect materials that are magnetic dipoles. The losses are approximately proportional to the frequency of the magnetic field and the square of the magnetic induction. The power of the hysteresis losses per unit volume is:

$$P_h = c_h\, B^2\, f \quad (3.11)$$

c_h is a material dependent constant. Selecting a material with soft magnetic properties can minimize the hysteresis losses.

Eddy current losses

Eddy currents are circular electric currents in a material induced by changing magnetic field. These currents are directly proportional to the square of the currents and the loss is:

$$P_E = c_E\, B^2\, f^2 \quad (3.12)$$

Resistive losses

The resistive losses in the coil windings are referred to as copper losses because the conductors are in most cases made of copper. Since copper is not magnetic dipole material, hysteresis loss will not appear. The resistive loss that appears in a conductor with electrical resistance R carrying a current I is:

$$P_c = I^2\, R \quad (3.13)$$

The efficiency is calculated as follows:

$$\square = \frac{Pout}{P\,in} \quad (3.14)$$

4. Work Done

4.1. Simulation of the Shock Absorber

In this project, the device was mathematically modeled using the above said equations and the results are tabulated as shown in Table 1.

The following assumptions, data and calculations were made before feeding it into the table.

1. The shock absorber is assumed to work in parasitic motions, which means the displacement of the coil relative to the stack is intermittent and not of a constant value. It calls for a simulated model which has two independent variables, speed of the vehicle and bump height.

2.

3. The Induced Voltage was calculated using the formula:

$$V = \pi \cdot N_w \cdot d_c \cdot v_{max} \cdot B_r / \sqrt{3} \qquad (4.1)$$

Induced Current was calculated using,

$$I = v_{max} \cdot A_w \cdot B_r \cdot \sigma / \sqrt{3} \qquad (4.2)$$

Power produced was calculated as,

$$P = V \cdot I \qquad (4.3)$$

4. The following data were collected before calculation

   Magnetic Induction of Neodymium magnets, $B_r = 0.03$ T

   Remanance, $c_h = 1.3$ T

   Eddy current factor, $c_E = 0.01724$ ohm.mm^2 / m

   Resistivity of Copper Wire, $(1/\sigma) = 58$ S.m/mm^2

   Length of the Wire, $l = 2.25$ m

   Number of turns, $N_w = 1540$

5. The velocity and the bump height modeling were based on the observation of the road conditions on a normal urban road. Table 4.1 shows the simulated values by inputting different bump heights and speeds.

Bump Height	Speed	Frequency	Induced voltage	Induced Current	Power Produced	Hyst
m	m/s	Hz	V	A	W	
0.05	12.5	50	2.942	0.9418	2.7715	0.
0.1	13	40	3.060	0.9794	2.9977	0.
0.15	14	30	3.295	1.0548	3.4766	0.
0.2	16	20	3.76684	1.205	4.5409	0.
0.25	18	10	4.23770	1.356	5.7471	0.

Table 4.1: Simulated data for power produced from Shock Absorber

Graphs were plotted for bump height vs. power output (Fig 4.1), power output vs. speed (Fig 4.2), induced voltage vs. speed (Fig 4.3), Induced current vs. bump height (Fig 4.4), bump height vs. power losses (Fig 4.5) and efficiency vs. bump height (Fig 4.6).

Fig 4.1: Power output W vs Bump Height
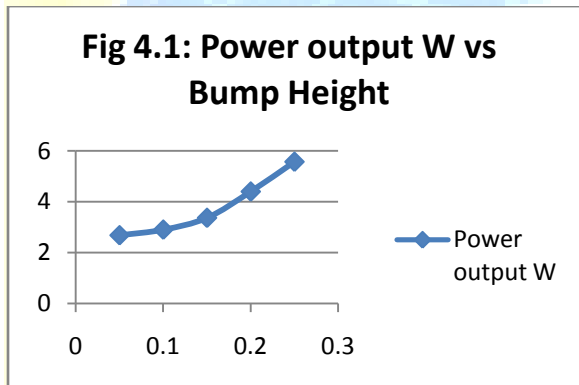
Fig 4.1 shows that the power output is increased with increase in bump height

Fig 4.2: Power output W vs Speed
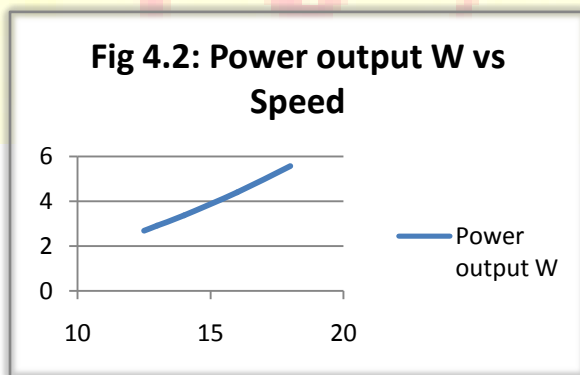
Fig 4.2 shows that the power output is increasing with increase in speed. We can observe an almost linear nature of the power output when speed increases
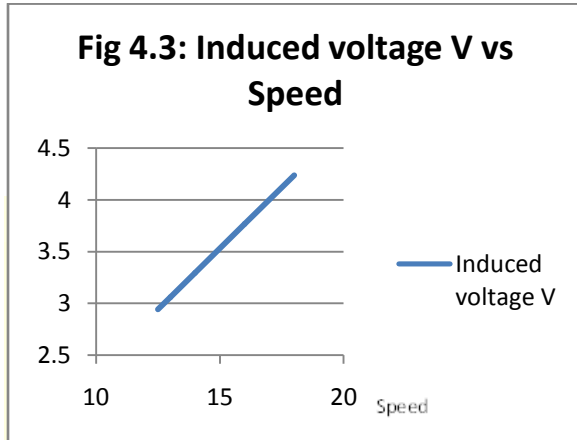

Fig 4.3: Induced voltage V vs Speed

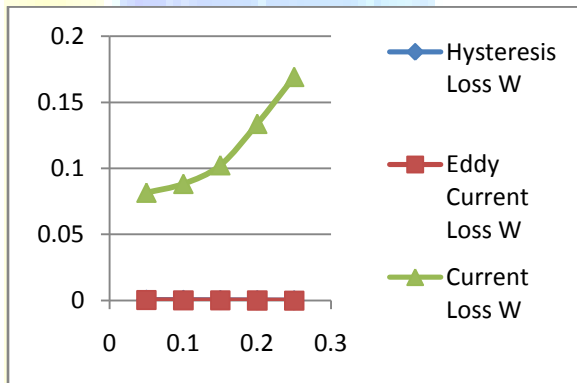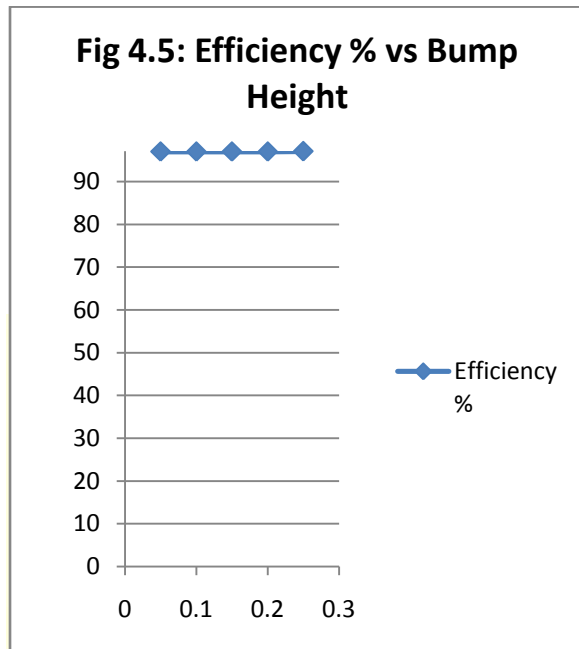Fig 4.3 shows that the induced voltage is a linear function of speed.

Fig 4.4 shows that the hysteresis loss and eddy current loss are almost constant and current loss increases exponentially with bump height, and thereby power production.

Fig 4.5: Efficiency % vs Bump Height

As we see from figure 4.5, the efficiency remains almost constant for the entire bump height range. The reason is, as the current production increases the resistive losses increases exponentially. So the efficiency is kept almost at a constant level.

Damping Factor:

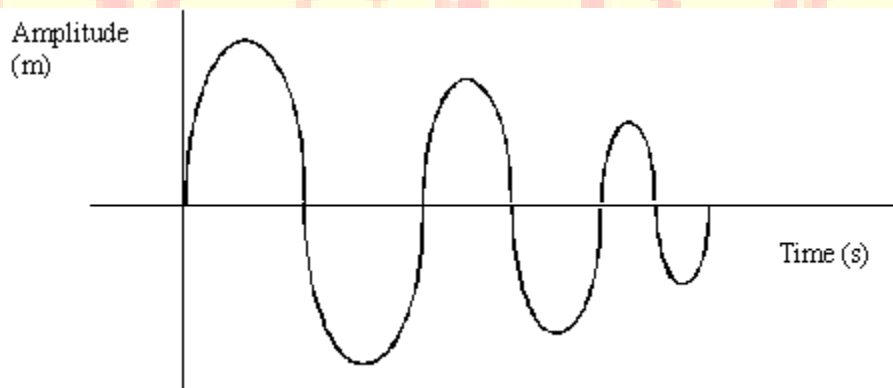A damping graph of a conventional shock absorber is shown:

Fig 4.7 showing the reducing ratio of a conventional Shock Absorber

From the table 4.1, the power produced is not 100%. So the input vibrational energy from the spring is not completely utilized, making it a under damped system. As of the simulation stage, a right tool to study the damping characteristics is not found but the energy conversion shows that the vibrations are damped by converting the mechanical energy to electrical energy.

4.2.Solid Modelling of the shock absorber

The design of the shock absorber was done using Pro E software according to the following specifications. Figure 4.8 and 4.9 shows the solid model of the RGSA.

Property	Value
Inner Stack magnet Dia	28 mm
Inner Stack Spacer Dia	28 mm
Outer coil Dia	28.2mm
Outer coil Support tube Outside Diameter	35 mm
Spring Diameter Inside	58 mm
Spring Diameter Outside	80 mm

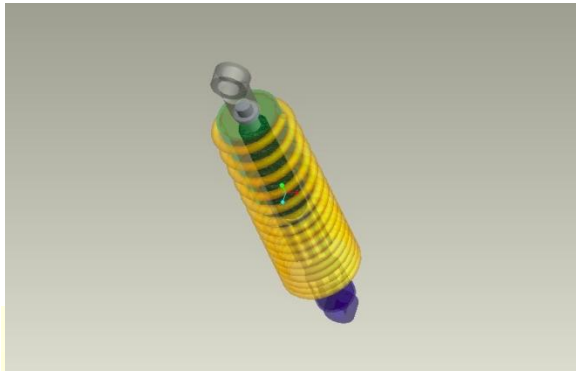*Fig 4.8: Pro E Design of the proposed device(Elevation)*

Fig 4.10: Perspective View showing the inner stack and outer coil

For the inner stack of magnets, Neodymium was used for the following advantageous properties as shown in table 4.2:

Property	Neodymium
Remanence (T)	1–1.3
Coercivity (MA/m)	0.875–1.99
Permeability	1.05
Temperature coefficient of remanence (%/K)	−0.12
Temperature coefficient of coercivity (%/K)	−0.55..–0.65
Curie temperature (°C)	320
Density (g/cm^3)	7.3–7.5
CTE, magnetizing direction (1/K)	5.2×10^{-6}
CTE, normal to magnetizing direction (1/K)	-0.8×10^{-6}
Flexural strength (N/mm^2)	250
Compressive strength (N/mm^2)	1100
Tensile strength (N/mm^2)	75
Vickers hardness (HV)	550–650
Electrical resistivity (Ω·cm)	$(110–170) \times 10^{-6}$

Table 4.2: Properties of Neodymium magnets

The spacers used were made up of stainless steel(SS), since SS is a diamagnetic material and it allows the magnetic field to pass through it.

The inner stack rod was made up of mild steel (MS), since mild steel gets attracted to magnet and helps in concentrating the axial magnetic field and also provides structural strength for the device.

The outer coil cover was also made up of SS and longitudinal slots milled to provide support to the coil.

The coil winding was made up of copper of thickness 0.977 mm. and runs for 2.25m length.

The outer spring was fabricated to suit this shock absorber dimensions and was made up of Mild Steel and the spring constant is roughly about 10000 N/m same as that of spring of **TVS Victor GX.**

4.3. Fabrication of the Shock Absorber

4.3.1 Magnetic Circuitry

The fabrication was carried out in the following sequence:

- Magnets were purchased for the following dimensions:

    Inner dia. = 15 mm

    Outer dia. = 28 mm

    Height of one magnet =10 mm

    Figure 4.11 shows the neodymium magnet.

Fig 4.11: A Sample Neodymium magnet

Mild steel rod was machined to the inner diameter of the magnet, i.e. 14.9mm. The stainless spacers (Fig 4.12) were then machined in a lathe to the same specification of that of the magnet and were arranged in a stack as shown in Figure 4.13.

Fig 4.12: A sample stainless steel spacer

Fig 4.13: Magnet Stack

- SS tube was first turned in a lathe for the specified diameter. The turning operation is shown in the Fig 4.14.

Fig 4.14: Turning Operation

- Longitudinal slots are then milled in the SS hollow tube which supports the coil winding. Fig 4.15 shows the milling operation and Fig 4.16 shows the finished operation.

Fig 4.15: Milling Operation

Fig 4.16: Finished Coil Support Tube

- An aluminum outer cover was provided outside the stack in order to shield the magnet and also to act as a dust cover. It was rough turned and then finished. (Fig 4.17)

Fig 4.18: Aluminum Dust Cover (After Turning)

- Since the existing **Victor GX** cannot be used since the overall radius of the damper is high, a new spring was fabricated for the same spring constant.

  It is forged component and the mild steel wire is cold drawn into spring.

Fig 4.19: Fabricated Spring for the vehicle

4.3.2 Electric Circuitry

The object of the electric circuit is to store the power produced by the shock absorber. The Shock Absorber produces intermittent AC voltage which must be rectified, standardized and then sent to storage in a battery.

So, a full wave rectifier was connected to the output terminal of the generator and then a capacitor for standardizing the power output.

The capacitor can then be connected to a battery of any voltage and it keeps building the voltage as long as it receives input from the shock absorber.
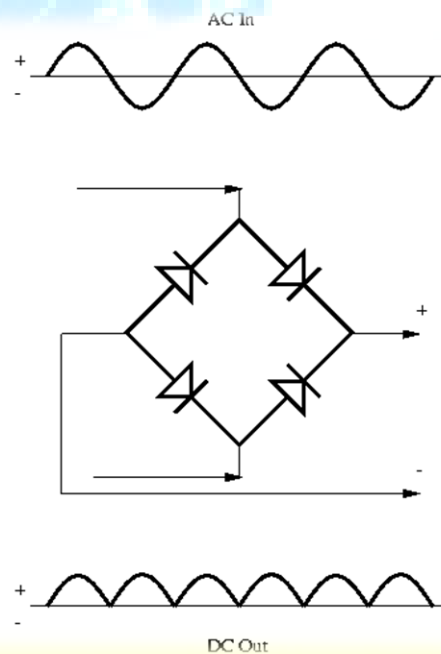
Fig 4.20: Full Wave Rectifier using normal silicon diode

The capacitor used for this purpose was 25 V, 4700 µF, which could store a large amount of charge.

4.4. Fitment in the bike

The bike used for the fitment of this shock Absorber was**Victor GX.** The existing spring arrangement was taken out by removing bolts on the frame and the wheel end. The photo of the bike with conventional shock absorber is shown in Fig 4.21 and without shock absorber is shown in Fig 4.22.

Fig 4.21: Bike with conventional Shock Absorber

Fig 4.22: Bike with Shock Absorber removed

The regenerative shock absorber was then fitted in the vehicle (Fig 4.23) with the stack as a stator and the coil as the rotor. That is, the coil was attached to the wheels and the magnet stack was attached to the frame.

Fig 4.23: Regenerative Shock Absorber attached to the vehicle

5.Experiments Conducted

The shock absorber fitted on the two wheeler vehicle was used as a test bench for conducting experiments. The vehicle was taken through different terrains and the displacement of the suspension (suspension travel) was noted and the terrain was reproduced by giving the movement to the device connected to the Oscilloscope.

The voltage curves were recorded using a Digital Storage Oscilloscope (DSO). Different terrains were reproduced in the form of bump height (displacement) and speed (frequency)and all the voltage vs. time curves were recorded as an image and the regeneration capacity of the shock absorber is studied. Fig 4.23 shows the test bench and Fig 5.1 shows the block diagram of theDigital Storage Oscilloscope.
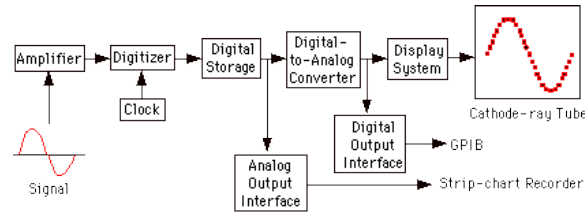
Fig 5.1: Block Diagram of Digital Storage Oscilloscope

6. Results and Discussions

The results of the experiment done on the test bench using the **Digital Storage Oscilloscope (DSO)** were stored in graphical form. The input is given in the form of displacement and frequency, which on real road conditions represent Bump Height and speed of the vehicle respectively.

6.1. Power Production under various road conditions

The device produces a maximum voltage of 2.5 V and a current of 15 mA under the maximum bump height conditions. Though we cannot expect the same voltage and power in normal roads, the device is able to generate voltages above 0.7 V consistently sending the generated power to the capacitor.

In all the following graphs the X axis represents time and Y axis represents voltage produced. The graphs were the image capture from the oscilloscope. Each graph represents a particular terrain and driving condition.The top right corner of the graph shows the scale of the X axis and the center box at the right shows the scale of the Y axis.
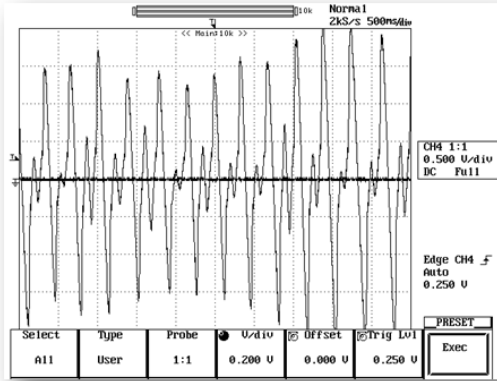
Fig 6.1: Variation of the voltage under off-road (rough) conditions

The above graph (Fig 6.1) shows the vehicle voltage curve under rough road conditions. The device alternately produces a peak voltage of 2 V consistently.
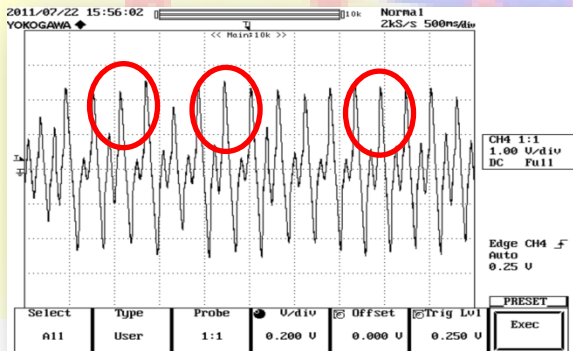

Fig 6.2: Off-Road Condition at a larger scale showing the peak voltage at 2.6 V

As we see from fig 6.2, that the device even reaches a voltage 2.6V under rougher conditions depending on the bump height and the speed of the vehicle.
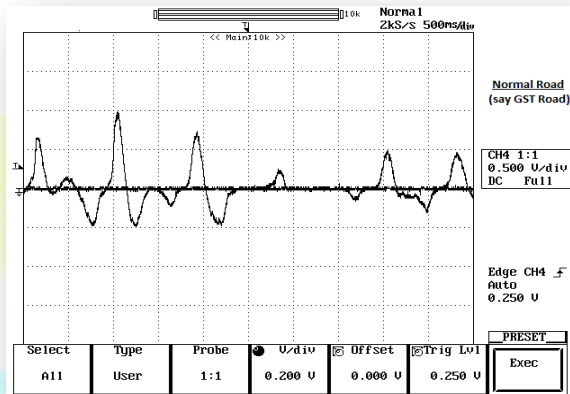

Fig 6.3: Voltage curve generated when vehicle is traversing in Highway

Fig 6.3 shows the performance of the device in highways. Though there won't be many bumps on the highways, we can't expect much power production from the device though it crosses the threshold 0.7V at some points.
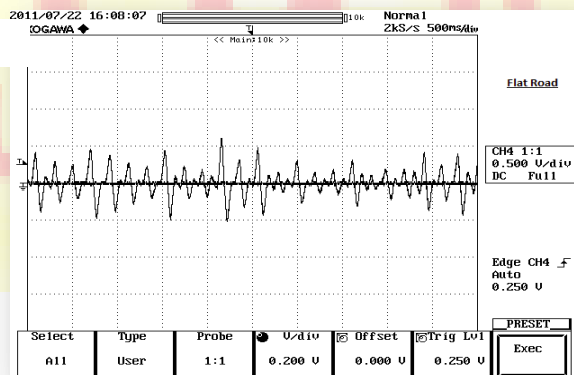

Fig 6.4: Voltage Curve on Highways, at a higher vehicle speed

Fig 6.4 shows the vehicle which is traversing the highway at a higher speed. We see frequent peaks but the voltage production is not on par with rough roads where the shock absorber is put to more use.
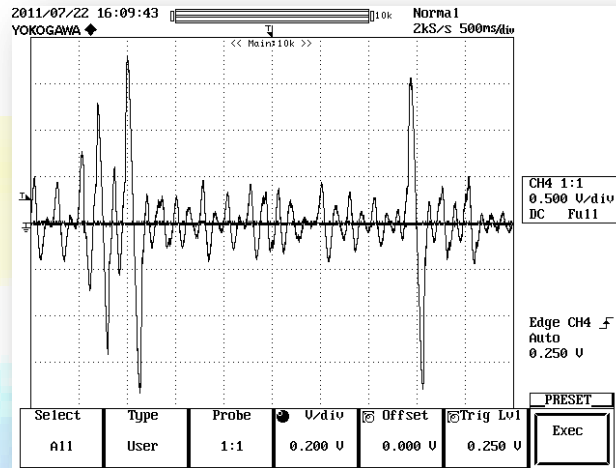

Fig 6.5: Voltage Production when the vehicle travels on the MIT College Road

Fig 6.5 shows the device performance on our college road, where there are two speed breakers at either end shown by the peaks in the graph.
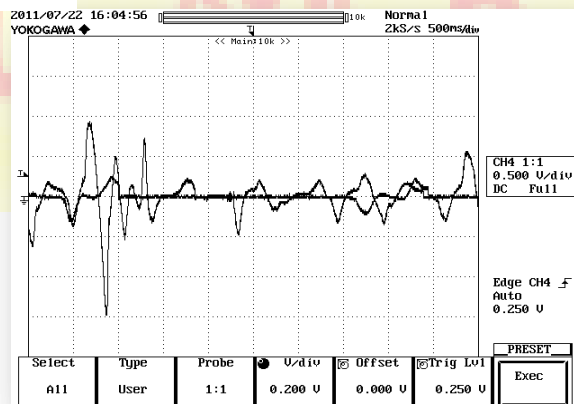

Fig 6.6: Variation of Voltage on Uneven Roads

Fig 6.6 shows the device's regeneration power capacity on an uneven road. As we see wherever there is a bump the device regenerates the wasted power. But the production of voltage is not even, the above fig justifies the usage of an electronic circuitry which standardizes the power.

The suspension not only compresses and elongates when it encounters a bump, but it does the same when the vehicle is accelerating or braking.

The following graphs (fig 6.7 and fig 6.8) show the voltage production of the device on a normal urban road which involves frequent braking and acceleration.
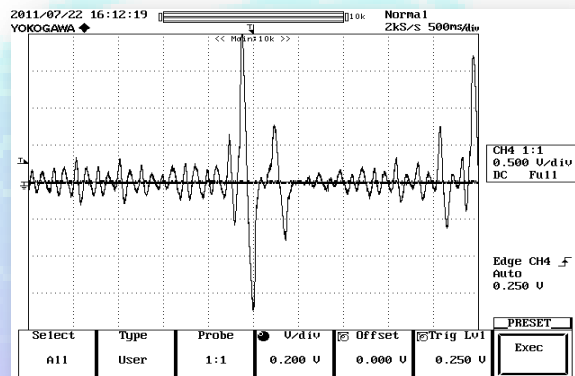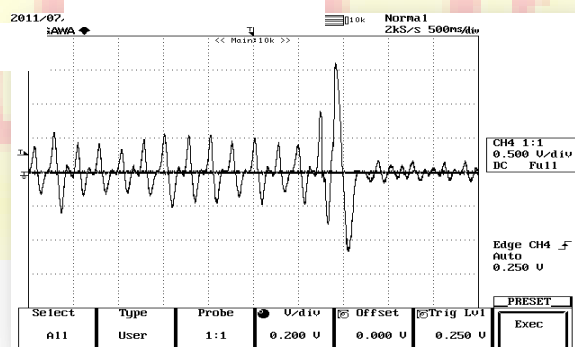

Fig 6.7: Effect of Acceleration on the suspension

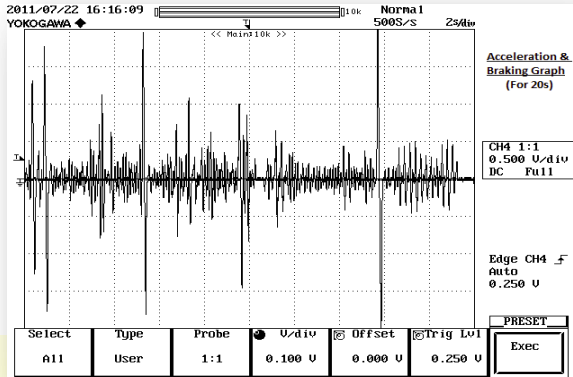

Fig 6.8: Effect of Smooth Braking

Fig 6.9: Working of the shock Absorber in urban conditions for 20s

The above graph is more a summary on the functioning of the regenerative shock absorber on a typical urban road travelling at a constant speed, acceleration and braking.

6.2 Damping Characteristics

The damping characteristics are studied through the voltage production by the existence of smaller peaks in subsequent cycles, although the bump has already crossed. The existence of the falling voltage peaks shows that the system is a under damped system, although the curve has to be smoothened out more than the conventional damper. The peak falls by a large value after the bump is encountered. As far as the ride comfort is concerned, no visible change between conventional and regenerative ride is felt.

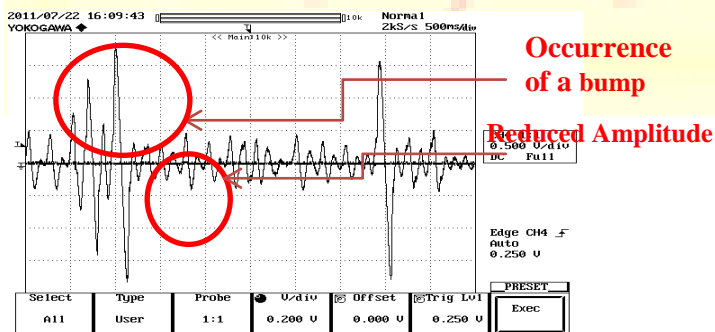Fig 6.10 shows the damping ratio after encountering a bump

Fig 6.10: Damping Effect of the device

6.3. Optimization

With the initial tests carried out, the following optimizations were tried and research was put into the device to maximize the power output and smoothening out the power.

- ✓ The SS spacers were replaced with Mild Steel Spacers in order that it also gets magnetized and the induction value B could increase and more flux lines could be produced.

- ✓ The magnets were stacked as a single unit without the spacers and the induced voltage is measured using the multimeter and it was found that the voltage remained the same with the magnet as a stack or spacers are kept in between. But, the former configuration is adopted so that the coil movement is present in the most magnetized area.

- ✓ The coil winding was done on a cardboard paper, which was not able to guide the stack and it kept falling on the coil present due to clearance between them. So, the coil is now wounded on a nylon sheet and the clearance is also reduced so that it could act as a guide. The voltage production was not disturbed by this action.

- ✓ In the electrical circuitry side, the full wave rectifier gave 1.4V drop across the diodes which inhibit the output power of the machine. So, a single diode rectifier was replaced, which gave 0.7V drop and the output power received from it was consistent.

- ✓ In order to increase the current production of the device, a higher rating wire diameter 0.977 m is used and the number of turns is increased.

- ✓ The aluminum outer cover is removed and the shock absorber is kept with just the coil and the magnet stack in order to reduce weight and the dust protection is given by the reduced clearance between the magnet and the coil. The voltage production remained the same.

A Monthly Double-Blind Peer Reviewed Refereed Open Access International e-Journal - Included in the International Serial Directories
Indexed & Listed at: Ulrich's Periodicals Directory ©, U.S.A., Open J-Gage as well as in Cabell's Directories of Publishing Opportunities, U.S.A.
International Journal of Management, IT and Engineering
http://www.ijmra.us

261

7.Conclusion

A regenerative shock absorber has been modeled and studied using a Digital Storage Oscilloscope and the following conclusions were made based on the results and discussions:

- The shock absorber is able to convert vibrational energy into useful electrical energy with a power rating of 6 W.
- The power produced by the shock absorber depends directly on the bump height.
- The shock absorber is highly efficient with an efficiency of 97%
- The device is highly useful in case of hybrid vehicles and could operate in sync with regenerative braking systems.

Improvisations and future works are suggested and references are given at the end of the report.

8. Future Works

The regenerative shock absorber project has the ability to expand its canvas to different domains of the suspension system. The following ideas and improvisations can be implemented and expanded:

Bump Height Sensor

The device has the inherent capacity to act as a sensor since the voltage produced is directly proportional to the bump height and it maintains a linear character making it suitable as a sensor. The bump height sensor can adjust the rear suspension of the vehicle as the front wheels already know the height of the bump, the rear wheels are going to encounter making the ride of a car more comfortable. This may eliminate the use of the accelerometer as the suspension also functions while acceleration and braking.

Robust Magnetic Circuitry

The neodymium magnets are costlier than Ferro magnets, but they are more advantageous in the production of magnetic field. Designs can be made such that power produced using normal magnets are sufficient enough for a mass produced vehicle narrowing the gap between conventional and regenerative shock absorbers. Also, the copper windings can be made with a higher current rated wire.

A Monthly Double-Blind Peer Reviewed Refereed Open Access International e-Journal - Included in the International Serial Directories
Indexed & Listed at: Ulrich's Periodicals Directory ©, U.S.A., Open J-Gage as well as in Cabell's Directories of Publishing Opportunities, U.S.A.

International Journal of Management, IT and Engineering
http://www.ijmra.us

262

All four wheels

If the shock absorber is used on all four wheels of the car or on all the four forks used in a two wheeler, it can be effective tool in reducing the carbon footprint. Design implications have to be faced and damping character should be more suitably tuned.

Electronic circuits

The silicon diode drops 0.7 V across it. This is a big value when compared with the voltage of 2.5 V. So the more advanced Schottkey diodes and a full wave rectifier can be used in place which drops just 0.6 V for a full wave rectifier almost doubling the power output.

9. References

1. *A Textbook of Electrical Technology ,B.L.Theraja , S. Chand Publications, ISBN : 9788121900997, Year Of Publication : 2010*

2. *Advanced Vehicle Technology, Heinz Heisler, Butterworth-Heinnmane, ISBN : 978812190099, 2002*

3. *United States Patent 6952060 Electromagnetic Linear Generator and Shock AbsorberGoldner, Ronald B. (Lexington, MA, US), Zerigian, Peter (Arlington, MA, US)*

4. *Analysis of Tubular-type Linear Generator for Free-Piston Engine, Dept. of Information & Control, 1† Dept. of Mechanics, Hoseo University, Baebang-myun,Asan, Chungnam, 336-795, KOREA*